Characterization of a Vertical Submersible Six-stage Pump: Accounting for the Induced Forces and Stresses

Patrick Zito Malonda[1], Guyh Dituba Ngoma[1], Walid Ghié[1], Fouad Erchiqui[1] and Python Kabeya[2]
[1]*University of Quebec in Abitibi-Témiscamingue, School of Engineering's Department, 445, Boulevard de l'Université, Rouyn-Noranda, Quebec, J9X 5E4, Canada*
[2]*University of Kinshasa, Department of Mechanical Engineering, Kinshasa, Democratic Republic of the Congo*

Keywords: Vertical Submersible Multistage Pump, Axial and Radial Forces, Stress, Strain, CFX, Static Structural Analysis.

Abstract: This study deals with the numerical investigation on the shaft behavior of a vertical submersible multistage pump in terms of the axial and radial forces, and the stresses due to the liquid flow through the pump while taking into account different conditions of operation, the gap between the impeller and the diffuser, the rotating speed and the number of stages. This is to improve the pump performances while selecting the bearings and/or the bushes of the submersible pumps in a suitable manner with a long operational life and high reliability. From an existing vertical submersible six-stage pump, a pump model is developed. The continuity, the Navier-Stokes, the stresses and the strains equations are applied to obtain by means of the ANSYS-codes the fields of the liquid flow velocity and the pressure, the stresses, the strains, so as the axial and radial forces. Numerical simulations are carried out to analyze the shaft behavior. The results obtained for the pump head and the stress are validated using the experimental results of the pump head and the results from the classical equations of stresses.

1 INTRODUCTION

The growth constantly of the number of deep mines in construction and in exploitation in Canada leads more and more to use very intense of the vertical submersible multistage pumps with high pressure in order to drain and to control the level of water in mines. The considered vertical submersible six-stage pump in this work is composed, inter alia, of a vertical shaft, six impellers, six diffusers, a motor, a suction body and a discharge body. The failing of a pump in a mine can have a very ominous impact on the environment. The security of the surrounding work environment depends extensively on its reliability, its good working and its life span. For the constructors of the hydraulic pumps, the design, the manufacture and the characterization of the vertical submersible multistage pumps always present a big challenge due to difficult to choose of the materials of the pump components; the performances to reach in terms of the pump head, the brake horsepower, the axial and radial loads, the stresses and the strains. A better manufacture of these pumps requires a determination with precision of all key parameters of its components while taking account, in the design phase the axial and radial loads, the strains and the stresses. Theoretical and experimental several research works have been achieved on the centrifugal pumps and the vertical submersible multistage pumps in tie with the axial and radial forces, the strains and the stresses on the pump shaft (Karassik, 1998; Gülich, 2010; Karassik et al., 2008; TM.P. S.p.A., 2003; Mohand-Amokrane Abdelouahab et al., 2020; Bin, et al., 2008; Zhou et al., 2014; Smith et al., 2005; Wang et al., 2013; Wang et al., 2014; and Suke et al., 2015). Indeed, in the books (Karassik, 1998; Gülich, 2010; Karassik et al., 2008; and TM.P. S.p.A., 2003), the authors presented theoretical and empiric approaches to calculate, among others, the axial and radial forces, the stresses and the strains on the shafts of the centrifugal and submersible pumps. It has been underlined that the developed relations are dependent of the types of pump including the measurements and the conditions of operations. They cannot be automatically generalized to all pumps. In the article (Mohand-Amokrane Abdelouahab et al., 2020), the authors studied

Malonda, P., Dituba Ngoma, G., Ghié, W., Erchiqui, F. and Kabeya, P.
Characterization of a Vertical Submersible Six-stage Pump: Accounting for the Induced Forces and Stresses.
DOI: 10.5220/0010551100920101
In *Proceedings of the 11th International Conference on Simulation and Modeling Methodologies, Technologies and Applications (SIMULTECH 2021)*, pages 92-101
ISBN: 978-989-758-528-9

numerically the axial and radial forces, the stresses and the strains on the shaft of a centrifugal four-stage pump in some function of the type of diffuser and the site of the diffuser to the last stage of pump. It has been demonstrated that the diffuser has an influence on the loads on the pump shaft. In the article (Smith et al., 2005), the authors have investigated on the vertical submersible turbine pumps (9 and 31 stages) to determine the axial forces, the stresses, the strains and the mechanical vibrations on the pump shaft. The influencing parameters on the loads have been identified. In the article (Wang et al., 2013), the authors worked on the optimization of the formula of calculation of the axial force in vertical submersible multistage pumps while taking into account the main liquid flows and leak flow through the pumps. This approach permitted to increase the precision in the determination of the axial force. The numerical results obtained have been compared with the experimental results to the ends of validation. The optimized formula gave some best results that the traditional formula of the axial force. In the article (Wang et al., 2014), the authors used the finite element method to calculate the stresses and the strains on the impellers of a vertical submersible four-stage pump. The effect of the thickness of the impeller blades on the stresses has been analyzed. Of what precedes and while widening the review of literature on the submersible pumps, it is to highlight that there is not research focused on the submersible pump that is considered in this research. In other words, the effects of the axial and radial forces, the strains and stresses on the performances of the investigated submersible pump have not been studied in the works of previous research. Failure to account for (or the underestimation) these elements in the design of the submersible can have negative impacts on the size of the pump shaft and its bearings (or the plain bearings) that are submitted to variable axial and radial loads according to the conditions of operation in terms of flow rates and rotating speeds. Besides, in most previous research works, the theoretical and empiric formulas to calculate the axial and radial forces on the shaft of pump have been elaborated in specific conditions in terms of components, measurements and operation of the pumps (Karassik, 1998; Gülich, 2010; Karassik et al., 2008; TM.P. S.p.A. , 2003; Bin, et al., 2008; Zhou et al., 2014; Smith et al., 2005; and Wang et al., 2013). Considering the features of different types of existing pumps, these formulas cannot be applied automatically in the case of the considered submersible pumps. Therefore, in this study, it is about developing reliable and precise numerical approach to determine the axial and radial forces, the strains and the stresses in the vertical submersible six-stage pump in while being based on the existing submersible pump. The numerical results achieved for the pump head and the stresses are compared with the experimental results and the results from classical equations of stresses.

2 MODEL DESCRIPTION

The vertical submersible six-stage pump considered as the reference pump for this work is illustrated in Fig. 1. It is composed, inter alia, of a shaft, six impellers and six diffusers.

The solid and the fluid models of this pump are shown in Fig. 2.

Figure 1: Vertical submersible six-stage pump (Technosub Inc., www.technosub.net).

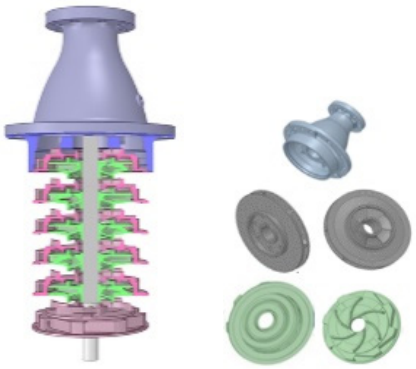

a) Solid model

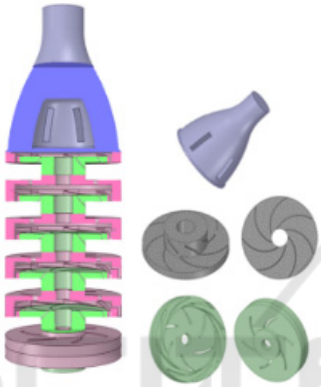

b) Fluid model

Figure 2: Model of a vertical submersible six-stage pump.

3 MATHEMATICAL FORMULATION

To determinate the field of the liquid flow velocity, the field of the pressure, the stress and the strain in a vertical submersible multistage pump, the following hypotheses are considered for the liquid flow (La Roche-Carrier et al., 2013), and the solid mechanics (Popov, 1999): (a) a steady state, three-dimensional and turbulence flow using the k-ε model is assumed; (b) the liquid is an incompressible liquid; (c) it is a Newtonian liquid; and (d) the liquid's thermophysical properties are constant with the temperature; (e) the material is considered continuous, doesn't have cracks, nor cavities; (f) the material is homogeneous and presents the same properties in all points; (g) the material is considered as isotropic; and (h) no internal force acts in the material before the application of the external loads.

3.1 Liquid Flow Velocity and Pressure

The equations of the continuity and the Navier-Stokes are used to obtain the fields of liquid flow velocity and pressure. These equations are solved by means of the ANSYS CFX-code (ANSYS inc.). The equation of the continuity is expressed as follows:

$$\frac{\partial u}{\partial x}+\frac{\partial v}{\partial y}+\frac{\partial w}{\partial z}=0 \tag{1}$$

where u(x,y,z), v(x,y,z) and w(x,y,z) are the components of the liquid flow velocity U(u,v,w).

Accounting for the gravity, the equations of the Navier-Stokes can be formulated by:

$$\begin{aligned}
&\rho\left(u\frac{\partial u}{\partial x}+v\frac{\partial u}{\partial y}+w\frac{\partial u}{\partial z}\right)=\mu_{eff}\left(\frac{\partial^2 u}{\partial x^2}+\frac{\partial^2 u}{\partial y^2}+\frac{\partial^2 u}{\partial z^2}\right)\\
&\qquad -\frac{\partial p}{\partial x}+\rho(\omega_z^2 r_x+2\omega_z v)+\rho g_x\\
&\rho\left(u\frac{\partial v}{\partial x}+v\frac{\partial v}{\partial y}+w\frac{\partial v}{\partial z}\right)=\mu_{eff}\left(\frac{\partial^2 v}{\partial x^2}+\frac{\partial^2 v}{\partial y^2}+\frac{\partial^2 v}{\partial z^2}\right)\\
&\qquad -\frac{\partial p}{\partial y}+\rho(\omega_z^2 r_y-2\omega_z u)+\rho g_y\\
&\rho\left(u\frac{\partial w}{\partial x}+v\frac{\partial w}{\partial y}+w\frac{\partial w}{\partial z}\right)=\mu_{eff}\left(\frac{\partial^2 w}{\partial x^2}+\frac{\partial^2 w}{\partial y^2}+\frac{\partial^2 w}{\partial z^2}\right)\\
&\qquad -\frac{\partial p}{\partial z}+\rho g_z
\end{aligned} \tag{2}$$

where g (g_x,g_y,g_z) ist the gravity acceleration, p is the pressure; ρ is the density; μ_{eff} is the effective viscosity accounting for turbulence, it is defined as $\mu_{eff}=\mu+\mu_t$. μ is the dynamic viscosity and μ_t is the turbulence viscosity. It is linked to turbulence kinetic energy k and dissipation ε (La Roche-Carrier et al., 2013).

3.2 Axial and Radial Forces

Fig. 3 illustrates the axial and radial forces due to the liquid flow through the vertical submersible six-stage pump which is considered in this research. These forces are determined using the ANSYS CFX-code. The axial forces are the result of unbalanced impeller forces acting in the shaft axial direction. Moreover, the radial force on the impeller results from a non-uniform distribution of pressure on the circumference of the impeller. The non-uniform pressure distribution can be caused by: the geometrical form of the diffuser for the multistage centrifugal pumps; the non-symmetrical impeller inflow; or the pump operating regime. It is to highlight that the radial force depends on the time. Its components are the static radial force and the dynamic radial force. Generally, the static radial force is greater than the dynamic

radial force (Abdelouahab, Mohand-Amokrane, et al., 2020; Karassik, 1998; Gülich, 2010; Wang et al., 2013; Watanabe, 2019; Gantar et al., 2002; Bolade et al., 2015;TM.P. S.p.A. Termomeccanica Pompe, 2003; Karassik et al., 2008; Jino, T., 1980).

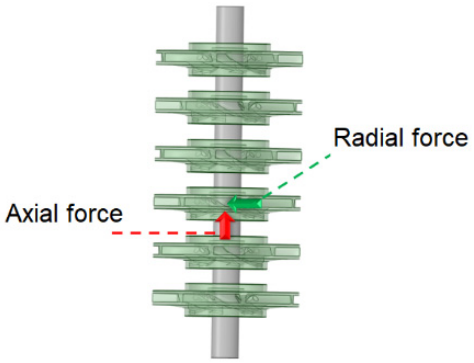

Figure 3: Axial and radial force in a model of the vertical submersible six-stage pump.

3.3 Stresses and Strains

The normal and the shear stresses on the pump shaft are determinated by means of the equilibrium equations of elasticity in terms of stress neglecting the forces per unit of volume (Popov, 1999). These equations are given by:

$$\begin{aligned}&\frac{\partial\sigma_x}{\partial x}+\frac{\partial\tau_{yx}}{\partial y}+\frac{\partial\tau_{zx}}{\partial z}=0\\&\frac{\partial\tau_{xy}}{\partial x}+\frac{\partial\sigma_y}{\partial y}+\frac{\partial\tau_{zy}}{\partial z}=0\\&\frac{\partial\tau_{xz}}{\partial x}+\frac{\partial\tau_{yz}}{\partial y}+\frac{\partial\sigma_z}{\partial z}=0\end{aligned}\tag{3}$$

The normal and the shear strains are formulated as follows using the displacements (u,v,w) respectively in the directions of x, y and z

$$\begin{aligned}&\varepsilon_x=\frac{\partial u}{\partial x};\ \varepsilon_y=\frac{\partial v}{\partial z};\ \varepsilon_z=\frac{\partial w}{\partial z}\\&\gamma_{xy}=\frac{\partial u}{\partial y}+\frac{\partial v}{\partial x};\ \gamma_{yz}=\frac{\partial w}{\partial y}+\frac{\partial v}{\partial z};\ \gamma_{zx}=\frac{\partial u}{\partial z}+\frac{\partial w}{\partial x}\end{aligned}\tag{4}$$

Furthermore, the relationships between the stresses and the strains is given by:

$$\begin{aligned}&\varepsilon_x=\frac{1}{E}\left[\sigma_x-\nu(\sigma_y+\sigma_z)\right]\\&\varepsilon_y=\frac{1}{E}\left[\sigma_y-\nu(\sigma_z+\sigma_x)\right]\\&\varepsilon_z=\frac{1}{E}\left[\sigma_z-\nu(\sigma_x+\sigma_y)\right]\\&\gamma_{xy}=\frac{\tau_{xy}}{G};\ \gamma_{yz}=\frac{\tau_{yz}}{G};\ \gamma_{zx}=\frac{\tau_{zx}}{G}\end{aligned}\tag{5}$$

where E is the modulus of elasticity, G is the shear modulus and ν is the Poisson's ratio.

In addition, the stresses can be written as the function of the strains by:

$$\begin{aligned}&\sigma_x=\frac{E}{(1+\nu)(1-2\nu)}\left[(1-\nu)\varepsilon_x+\nu(\varepsilon_y+\varepsilon_z)\right]\\&\sigma_y=\frac{E}{(1+\nu)(1-2\nu)}\left[(1-\nu)\varepsilon_y+\nu(\varepsilon_z+\varepsilon_x)\right]\\&\sigma_z=\frac{E}{(1+\nu)(1-2\nu)}\left[(1-\nu)\varepsilon_z+\nu(\varepsilon_x+\varepsilon_y)\right]\\&\tau_{xy}=G\gamma_{xy};\ \ \tau_{yz}=G\gamma_{yz};\ \ \tau_{zx}=G\gamma_{zx}\end{aligned}\tag{6}$$

The stress of von Mises selected for the yield criteria can be expressed by:

$$\sigma'=\sqrt{\frac{1}{2}\left(\left(\sigma_1-\sigma_2\right)^2+\left(\sigma_2-\sigma_3\right)^2+\left(\sigma_3-\sigma_1\right)^2\right)}\tag{7}$$

where σ_1, σ_2 and σ_3, are the principal stresses in the directions of 1, 2 and 3 according to $\sigma_1 > \sigma_2 > \sigma_3$. These stresses can be determined as follows (Popov, 1999):

$$\begin{aligned}&\sigma_1=\sigma_0+2\left(\left|\frac{J_2}{3}\right|\right)^{\frac{1}{2}}\cos\left(\frac{1}{3}\arccos\left(-0.5J_3\left(\left|\frac{J_2}{3}\right|\right)^{-1.5}\right)\right)\\&\sigma_2=\sigma_0-2\left(\left|\frac{J_2}{3}\right|\right)^{\frac{1}{2}}\cos\left(\frac{1}{3}\arccos\left(-0.5J_3\left(\left|\frac{J_2}{3}\right|\right)^{-1.5}\right)+\frac{\pi}{3}\right)\\&\sigma_3=\sigma_0-2\left(\left|\frac{J_2}{3}\right|\right)^{\frac{1}{2}}\cos\left(\frac{1}{3}\arccos\left(-0.5J_3\left(\left|\frac{J_2}{3}\right|\right)^{-1.5}\right)-\frac{\pi}{3}\right)\end{aligned}\tag{8}$$

Where

$$\begin{aligned}&\sigma_0=\frac{1}{3}\left(\sigma_x+\sigma_y+\sigma_z\right)\\&J_2=s_xs_y+s_ys_z+s_zs_x-\tau_{xy}^2-\tau_{yz}^2-\tau_{zx}^2\\&J_3=-\left(s_xs_ys_z-s_x\tau_{yz}^2-s_y\tau_{zx}^2-s_z\tau_{xy}^2\right)\\&s_x=\sigma_x-\sigma_0;\ \ s_y=\sigma_y-\sigma_0;\ \ s_z=\sigma_z-\sigma_0\end{aligned}\tag{9}$$

3.4 Diffuser Equations

The diffuser equations (Gülich, J. F., 2010) are used in this research to calculate the main parameter of the diffusers of the vertical submersible six-stage pump as illustrated in Fig. 4.

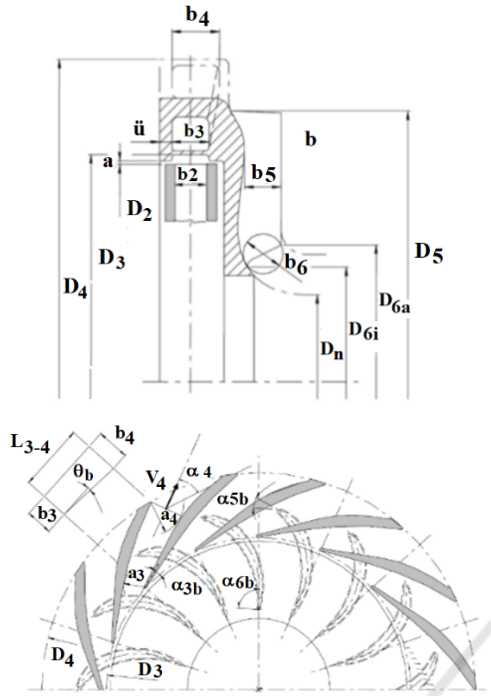

Figure 4: Diffuser parameters (Gülich, J. F., 2010).

These equations can be formulated as follows:

$$b_3 = (1.05 \text{ to } 1.3)\cdot b_2 \tag{10}$$

$$\alpha_{3b} = \alpha_3 \pm 3^{\circ} \text{ and } \alpha_3 = \tan^{-1}\left(\frac{V_{m3}}{V_{u3}}\right) \tag{11}$$

$$V_{m3} = \frac{Q \cdot \tau_3}{\pi \cdot D_3 \cdot b_3} \tag{12}$$

$$V_{u3} = V_{u2} \cdot \left(\frac{D_2}{D_3}\right) \tag{13}$$

$$V_{u2} = \frac{gH}{\eta_h U_2} + \frac{U_{1m} V_{1u}}{U_2} \tag{14}$$

$$a_3 = f_{a3} \cdot \left(\frac{D_3}{2}\right) \cdot \left\{ \exp\left[\frac{Q}{b_3 \cdot V_{2u} \cdot \left(\frac{D_2}{2}\right) \cdot Z_{Le}} \right] - 1 \right\} \tag{15}$$

where $1.1 \le f_{a3} \le 1.3$, the vane number of the diffuser Z_{Le} is chosen according to Tab. 1.

Table 1: Number of blades required for the diffuser (Gülich, J. F., 2010).

Z_b	5			6	7				
Z_{Le}	7	8	12	10	9	10	11	12	(15)

$$e_3 = (0.01 \text{ à } 0.015)\cdot D_2 \tag{16}$$

$$D_4 = ((1.05 \text{ à } 1.15) + 0.01 \cdot n_q)\cdot D_2 \tag{17}$$

where n_q is the specific speed.

$$\vartheta_b = \tan^{-1}\left(\frac{0.5\cdot(a_4 - a_3)}{L_{3-4}}\right) \tag{18}$$

$$b_4 = b_3 + (\tan(\vartheta_b)\cdot L_{3-4}) \tag{19}$$

$$b_5 = b_6 = \frac{Q}{\pi \cdot D_6 \cdot V_{m6}} \tag{20}$$

$$V_{m6} = (0.85 \text{ à } 0.9)\cdot V_{m1} \tag{21}$$

$$\alpha_5 = \tan^{-1}\left(\frac{V_{m5}}{V_{u5}}\right) \tag{22}$$

$$V_{m5} = \frac{Q}{\pi \cdot D_5 \cdot b_5} \tag{23}$$

$$V_{u5} = V_{u4} \cdot \left(\frac{D_4}{D_5}\right) \tag{24}$$

$$V_{u4} = V_{u3} \cdot \left(\frac{D_3}{D_4}\right) \tag{25}$$

$$\alpha_{6b} = \alpha_6 \pm 5^{\circ} \tag{26}$$

Moreover, Fig. 5 indicates the boundary conditions used in this work. Indeed, at the pump inlet, the static pressure is specified, while the flow rate is given at the pump outlet. For the interaction of the impeller-diffuser, the frozen rotor condition is applied.

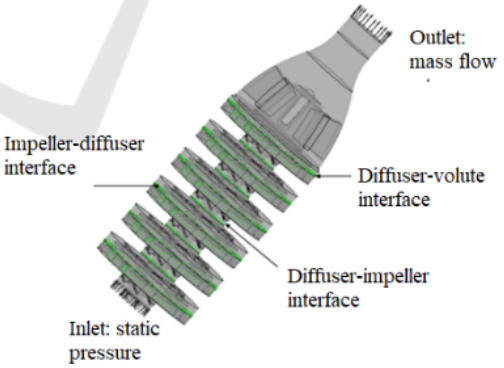

Figure 5: Boundary conditions for the vertical submersible six-stage pump.

4 RESULTS AND DISCUSSION

To study the shaft behavior in terms of the axial and radial forces, and the stresses, three key parameters were selected: (a) the intensity of the impeller

trimming (100 %, 91.7%, and 84.65 %); (b) the number of the stages (4, 5 and 6 stages); and (c) the shaft rotating speed (1800 rpm and 3600 rpm). According the numerical results obtained, different numbers of mesh elements are used in each case study to achieve the mesh-independent solution tests. The reference data applied for the shaft, the impeller, and the diffuser are given in Tabs. 2-5.

Table 2: Pump shaft data.

Length L [mm]	655,15
Diameter d [mm]	45,06

Table 3: Impeller data.

Inlet blade height b_1 [mm]	30.17
Outlet blade height b_2 [mm]	14.48
Hub diameter D_{h1} [mm]	44,45
Inlet diameter D_{h2} [mm]	107.95
Outlet diameter D_2 [mm]	241
Inlet blade angle β_{b1} [°]	16
Outlet blade angle β_{b2} [°]	27.5
Blade thickness e [mm]	3.17
Blade number Z_b	7

Table 4: Diffuser (front side) data.

Inlet blade height b_3 [mm]	17.46
Outlet blade height b_4 [mm]	40.64
Inlet diameter D_3 [mm]	243,84
Outlet diameter D_4 [mm]	311.15
Inlet blade angle α_{3b} [°]	10
Blade thickness e_3 [mm]	3.175
Blade number Z_{Le}	8

Table 5: Diffuser (rear side) data.

Return vane number Z_R	6
Outlet return vane height b_5 [mm]	24,4
Diameter at the inlet of the return vane D_3 [mm]	311,15
Blade angle at the inlet of the return vane α_5 [°]	95
Blade angle at the outlet of the return vane α_6 [°]	18
Blade thickness of the return vane e_3 [mm]	6,04

In addition, the properties of the 17-4PH steel and the water considered are continued in Tabs. 6 and 7.

Table 6: Properties of the 17-4PH steel.

Module of the Young [Pa]	$1,96x10^{11}$
Poisson ratio	0,3
Compressibility module [Pa]	$1,63x10^{11}$
Shear module [Pa]	$7,53x10^{10}$
Resistance coefficient [Pa]	$9,2x10^{8}$
Ductility coefficient [Pa]	10^{9}
Yield strength [Pa]	$7.93x10^{8}$
Ultimate tensile strength [Pa]	$1.103x10^{9}$
Density [kg/m^3]	7750,4

Table 7: Properties of water in 25 °C.

Density [kg/m^3]	Thermal expansion coefficient [K^{-1}]	Kinematic viscosity [m^2/s]
997	$2,57x10^{-1}$	$0,884x10^{-6}$

4.1 Case Study

4.1.1 Effect of the Impeller Trimming

To examine the effect of the variation of the impeller diameter on the performances of the vertical submersible six-stage pump, three impeller diameter ratios of the 100 % (corresponding to the reference impeller diameter: 241 mm), 91.7 % and 84.65 % were selected when keeping other parameters constant. Fig. 6 shows the pump head as a function of the flow rate. From this figure, it can be seen that the pump head decreases with the reduction of the impeller diameter ratio. This can be explained by the fact that the pressure difference between the impeller outlet and inlet decreases with decreasing impeller diameter ratio maintaining the diffuser inner diameter constant. The energy of the fluid generated by the rotating impeller was affected by the impeller trimming which modifies the blade angle. In addition, Fig. 7 indicates that the brake horsepower diminishes with the reduction of the impeller diameter ratio due to the requested diminution impeller shaft torque relative to the size of the impeller diameter keeping the diffuser inner diameter constant. Furthermore, the corresponding efficiency curves as a function of the flow rate illustrated in Fig. 8 shows that the efficiency is the best for the lowest impeller trimming. Moreover, Figs. 9-11 show that the impeller trimming decrease the axial force, the radial force and the stress on the pump shaft. It may be due to the interaction between the impeller and the diffuser, that is reduced by the decrease of the impeller diameter.

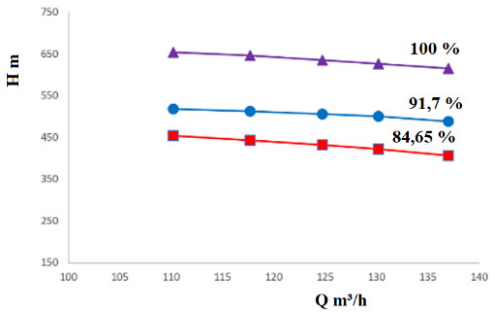

Figure 6: Head versus flow rate.

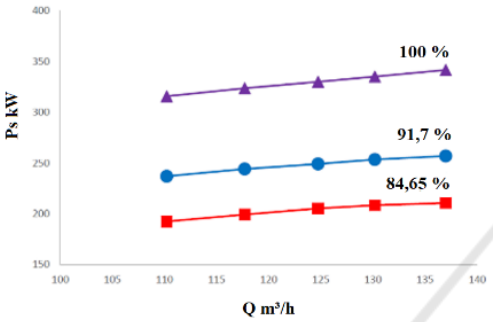

Figure 7: Brake horsepower versus flow rate.

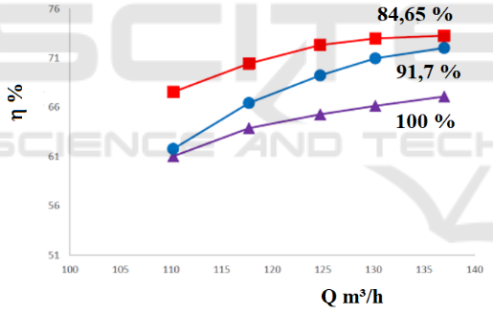

Figure 8: Efficiency versus flow rate.

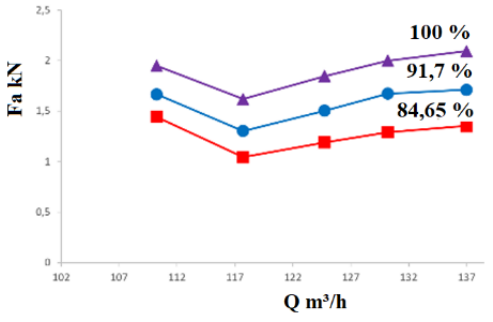

Figure 9: Axial force versus flow rate.

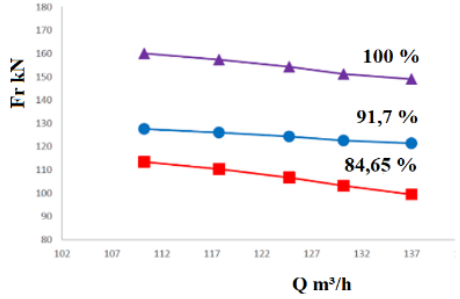

Figure 10: Radial force versus flow rate.

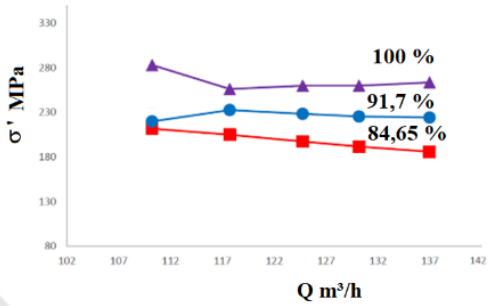

Figure 11: Stress versus flow rate.

4.1.2 Effect of Number of the Stages

To examine the effect of the stage number on the pump shaft behavior, three pumps with 3, 5 and 6 stages are selected. Figs. 12-17 provide some relevant information on the influence of the number of the pump stages on the pump performances, the axial and radial forces, and the stress. More the number of the stages is raised, more the pump head is important as shown in the Fig. 12. The brake horsepower increases with decreasing the number of the pump stages as indicated in Fig. 13, whereas the efficiency is unchanged despite the number of the pump stages as shown in Fig. 14. In addition, It can see in Figs. 15-17 that the axial and radial forces, and the stress diminish with decreasing the number of the pump stages.

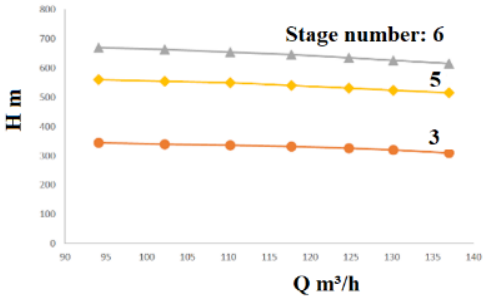

Figure 12: Head versus flow rate.

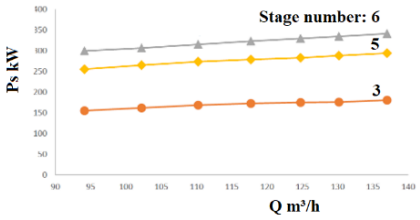

Figure 13: Brake horsepower versus flow rate.

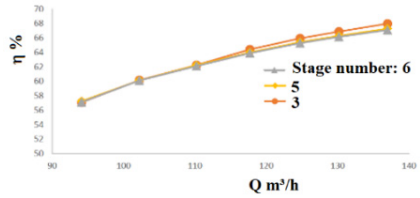

Figure 14: Efficiency versus flow rate.

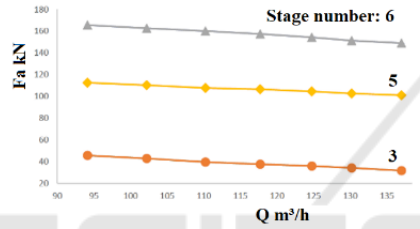

Figure 15: Axial force versus flow rate.

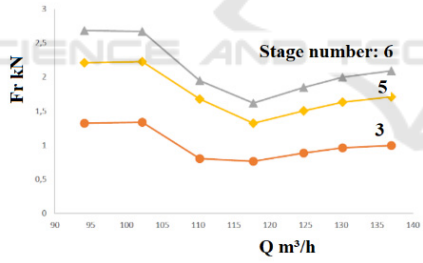

Figure 16: Radial force versus flow rate.

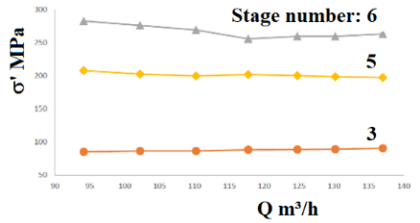

Figure 17: Stress versus flow rate.

4.1.3 Effect of the Shaft Rotating Speed

This analysis concentrates on the effects of the shaft rotation speed on the performances of the vertical submersible six-stage pump accounting for the induced forces and the stresses on the shaft. Selecting the rotating speeds of 1800 rpm and 3600 rpm, Figs. 18-23 show that the pump head and the brake horsepower grow with increasing the rotation speed, whereas the efficiency increase and decreases with the rotation speed in the considered flow rate range. Moreover, Fig. 21 and 22 indicate that respectively the axial and radial forces increase with the augmentation of the rotating speed. In regard to the stress on the pump shaft, it raises with the growing of the rotating speed as depicted in Fig. 23.

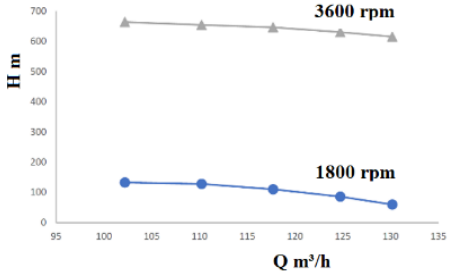

Figure 18: Head versus flow rate.

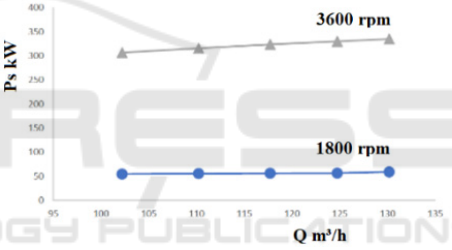

Figure 19: Brake horsepower versus flow rate.

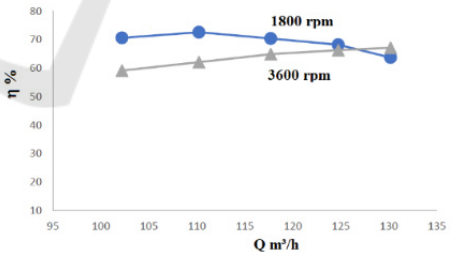

Figure 20: Efficiency versus flow rate.

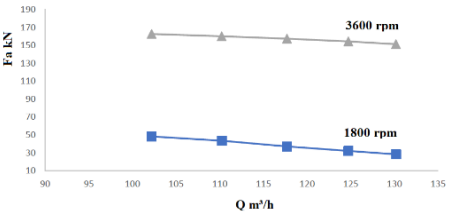

Figure 21: Axial force versus flow rate.

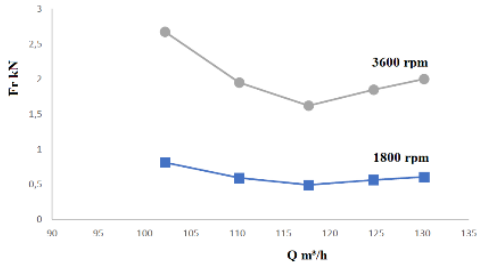

Figure 22: Radial force versus flow rate.

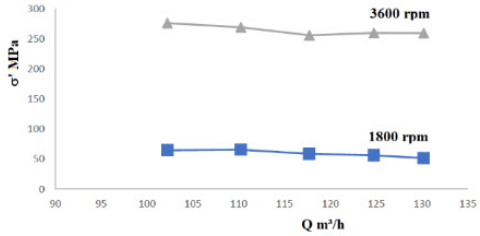

Figure 23: Stress versus flow rate.

4.2 Comparison of the Results

The numerical results of the head for a vertical submersible six-stage pump are compared with the experimental results to validate the developed approach as depicted in Fig. 24. A good agreement was observed between both curves.

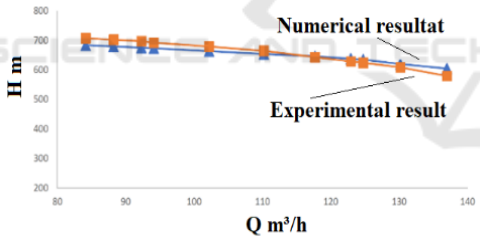

Figure 24: Head versus flow rate.

In addition, the stresses obtained on the pump shaft (one-stage pump) using the numerical simulations and the classical equations are confronted as illustrated in Fig. 25. This comparison shows good harmony.

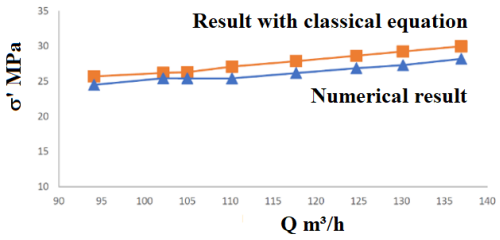

Figure 25: Stress versus flow rate.

5 CONCLUSION

In this work, the pump shaft behavior of a vertical submersible multistage pump was numerically investigated in terms of the axial and radial forces, and the stresses due to the liquid flow through the pump while taking into account different conditions of flow operation. The effects of three key parameters such as the impeller trimming, the rotating speed and the number of stages on the pump performances were analyzed by means of the ANSYS-codes. The simulation results achieved reveal, inter alia, the existence of strong relationships between the pump performances, the axial and radial loads, and the stresses on the shaft varying the number of stages, the rotating speed and the intensity of the impeller trimming. This could be considered to improve the pump performances while selecting the bearings and/or the bushes of the vertical submersible six-stage pumps in a suitable manner with a long operational life and high reliability. Finally, the obtained numerical results for the pump head and the stresses on the shaft are compared respectively with the experimental results and the results using the classical equations of stresses.

ACKNOWLEDGMENTS

The authors are grateful to the Technosub Inc., Industrial pumps manufacturing and distribution (Rouyn-Noranda, Quebec, Canada).

REFERECES

Karassik, I. J., McGuire, T., 1998. *Centrifugal Pumps*. Springer-Verlag US.

Gülich, J. F., 2010. Centrifugal Pumps, second Edition, Springer.

Karassik, I. J., Messina, J. P., Cooper, P., Heald, C. C., 2008. Pump Handbook. Fourth edition McGRAW-HILL.

TM.P. S.p.A. Termomeccanica Pompe, 2003. TERMOMECCANICA Centrifugal pump handbook, La Spezia – Italy.

Abdelouahab, M. A., Guyh Dituba Ngoma. G., Erchiqui, F., Kabeya, P.(2020), Numerical Study of the Axial and Radial Forces, the Stresses and the Strains in a High Pressure Multistage Centrifugal Pump. 10th International Conference on Simulation and Modeling Methodologies, Technologies and Applications (SIMULTECH). Online streaming, 8-10 juillet.

Xia, B., Kong, F., Zhang, H., Yang, L., and Qian, W., 2018. Investigation of axial thrust deviation between the theory and experiment for high-speed mine submersible pump. Advances in Mechanical Engineering, Vol. 10(8) 1–13.

Zhou L., Shi W.D., Bai L., Lu W.G. and Li W., 2014 Numerical calculation and experimental study of axial

force in a deep-well centrifugal pump. Lat. Am. appl. res. vol.44 no.1, Bahía Blanca ene.

Smith, D. R.; Price, S., 2005. Upthrust Problems On Multistage Vertical Turbine Pumps. Turbomachinery and Pump Symposia.

Wang C., Shi, W. and Zhang, L., 2013. Calculation Formula Optimization and Effect of Ring Clearance on Axial Force of Multistage Pump. Hindawi Publishing Corporation, Mathematical Problems in Engineering, Vol. 2013, Article ID 749375.

Wang, C., Shi, W., Si, Q., Zhou, L., 2014. Numerical calculation and finite element calculation on impeller of stainless steel multistage centrifugal pump. Journal of Vibroengineering, Vol. 16, Issue 4, p. 1723-1734.

Suke, A. C., Londhe, B. P., Verma, A. B., 2015. Shaft deflection Analysis of Multistage centrifugal Pump by Finite element Method. International Journal of Science, Engineering and Technology Research, Vol. 4, Issue 7.

Technosub Inc., www.technosub.net.

Bolleter, U., Frei, A., 1993. Shaft Sizing for Multistage Pumps. Turbomachinery Laboratories, Department of Mechanical Engineering, Proceedings of the tenth international pump users symposium.

Popov E. P., 1999. Engineering Mechanics of Solids, 2nd edition, Prentice Hall.

La Roche-Carrier N., Dituba Ngoma G., and Ghie W., 2013. Numerical investigation of a first stage of a multistage centrifugal pump: impeller, diffuser with return vanes, and casing. ISRN Mechanical Engineering, Vol. 2013, Article ID 578072, 15 pages.

Gantar M., Florjancic D., and Sirok B., 2002. Hydraulic Axial Thrust in Multistage Pumps - Origins and Solutions. Journal Fluids Engineering, Vol. 124, Issue 2, 336-341, 6 pages.

Bolade, P. S., Madki, S. J., 2015. Analysis of Hydraulic Thrusts in Centrifugal Pump to Increase the Bearing Life. International Journal of Engineering Research & Technology. ISSN: 2278-0181, Vol. 4 Issue 08.

Jino, T., 1980. Hydraulic axial thrust in multistage centrifugal pumps. Journal of Fluids Engineering, Volume 102, Issue 1, 6 pages.

Karassik, I. J., Messina, J. P., Cooper, P., Heald, C. C., 2008. Pump Handbook. Fourth edition McGRAW-HILL.

ANSYS inc., www.ansys.com.